JACS
JOURNAL OF THE AMERICAN CHEMICAL SOCIETY
pubs.acs.org/JACS
Communication

Light-Powered Reversible Guest Release and Uptake from Zn_4L_4 Capsules

Amit Ghosh, Laura Slappendel, Bao-Nguyen T. Nguyen, Larissa K. S. von Krbek, Tanya K. Ronson, Ana M. Castilla, and Jonathan R. Nitschke*

Cite This: *J. Am. Chem. Soc.* 2023, 145, 3828–3832

Read Online

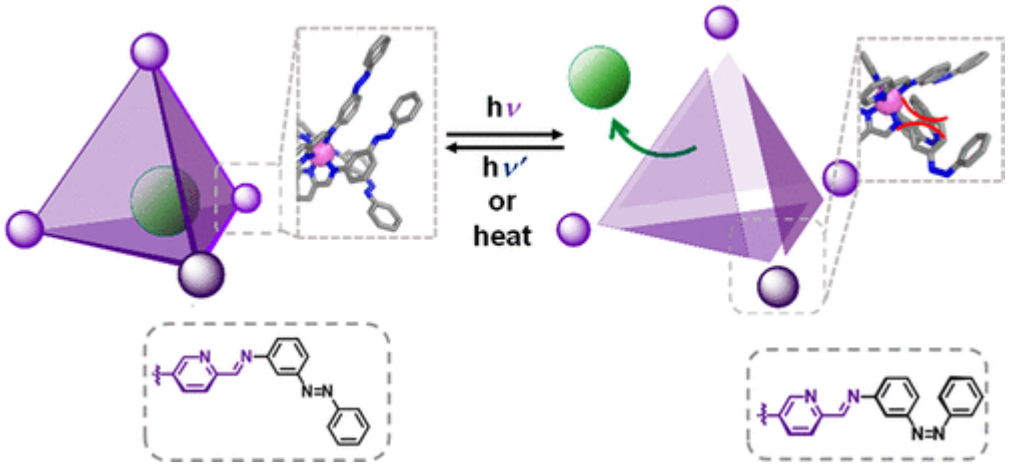

Subcomponent B

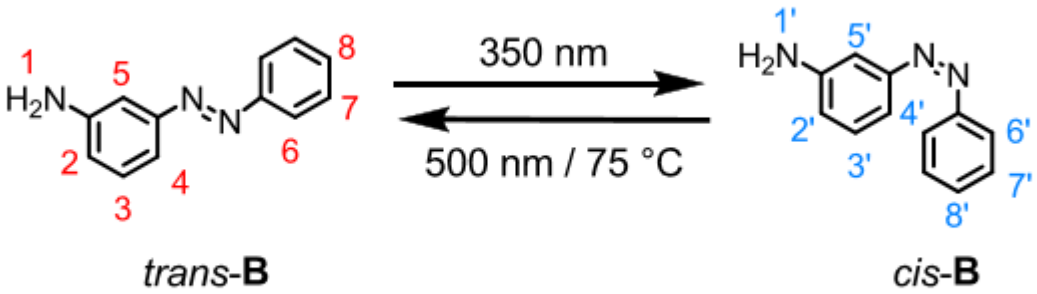

Figure S20. Reversible photoswitching of azobenzene-containing subcomponent **B.**

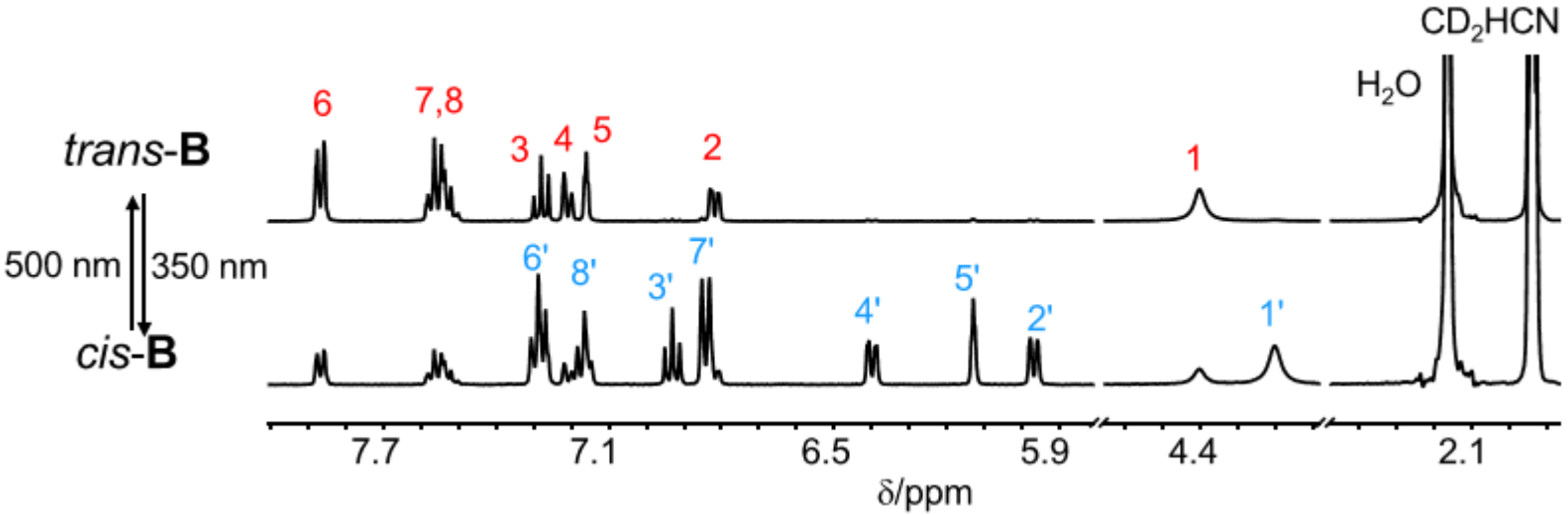

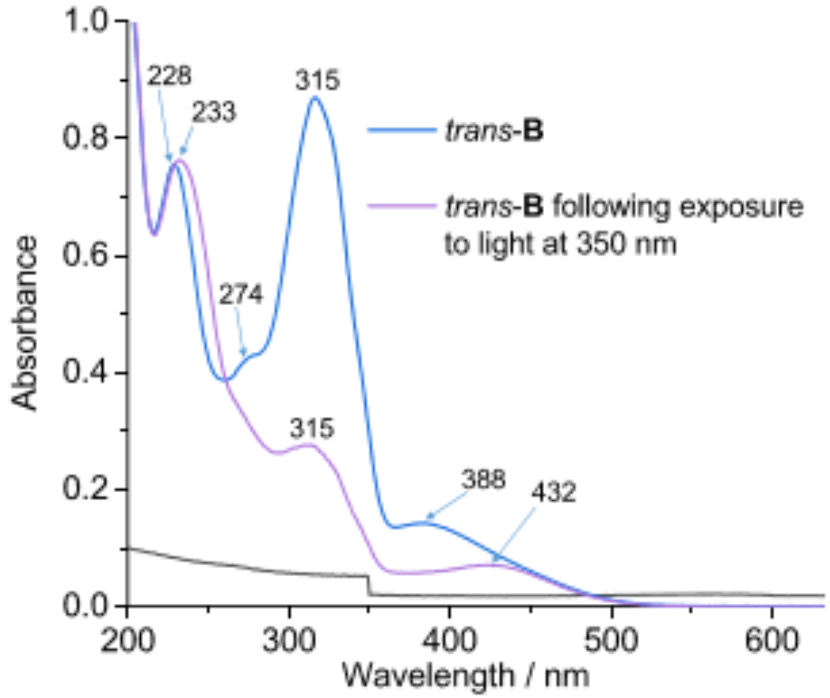

Figure S24. The comparison of the UV-vis spectra of *trans*-**B** (7.2×10^{-6} M, CH_3CN, 25 °C) and then following exposure to light at 350 nm for 10 min.

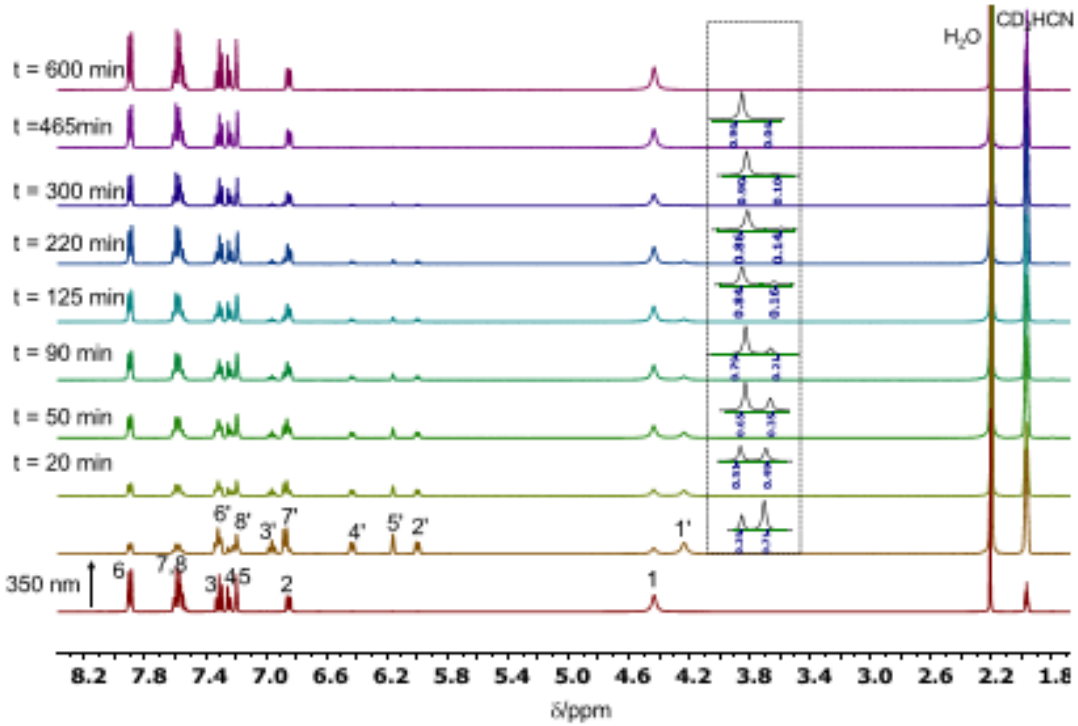

Figure S22. Time-dependent ^{1}H NMR (CD_3CN, 400 MHz, 25 °C) spectrum monitoring interconversion between *cis*-**B** to *trans*-**B** by heating the solution at 75 °C.

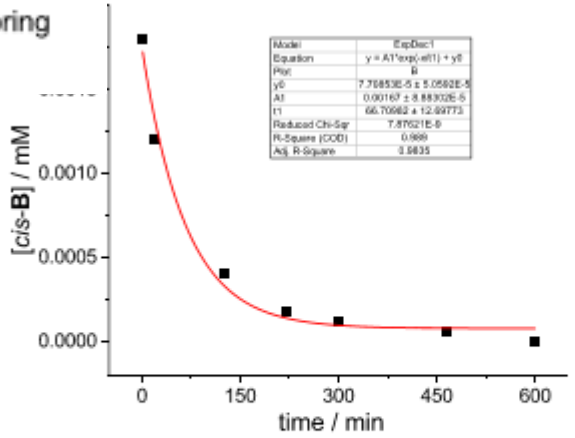

Figure S23. Kinetics for the *cis* to *trans* isomerisation of ligand **B** at 75 °C, monitored by the relative integration of protons 1 and 1' in the ^{1}H NMR (Figure S17). The fitting following a 1st order kinetics (red line), revealing a half-life of $t_{1/2}$ = 46 min and rate constants of k = 2.5 x 10^{-4} s^{-1}.

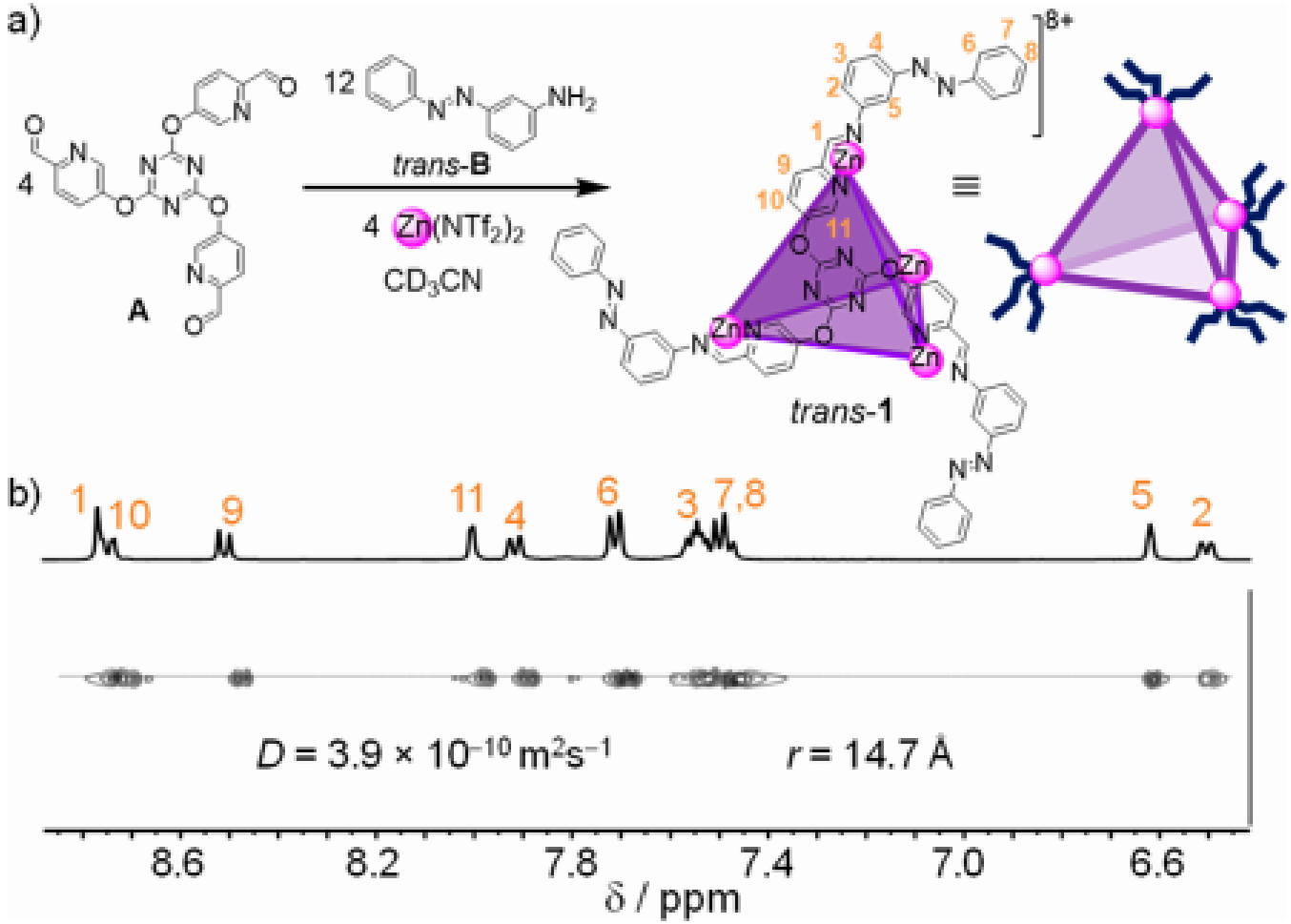

Figure 1. a) Assembly of subcomponents **A** and *trans*-**B** with Zn^{II} produced cage *trans*-**1**. b) ^{1}H and DOSY NMR (400 MHz, CD_3CN, 298 K) spectra of *trans*-**1**.

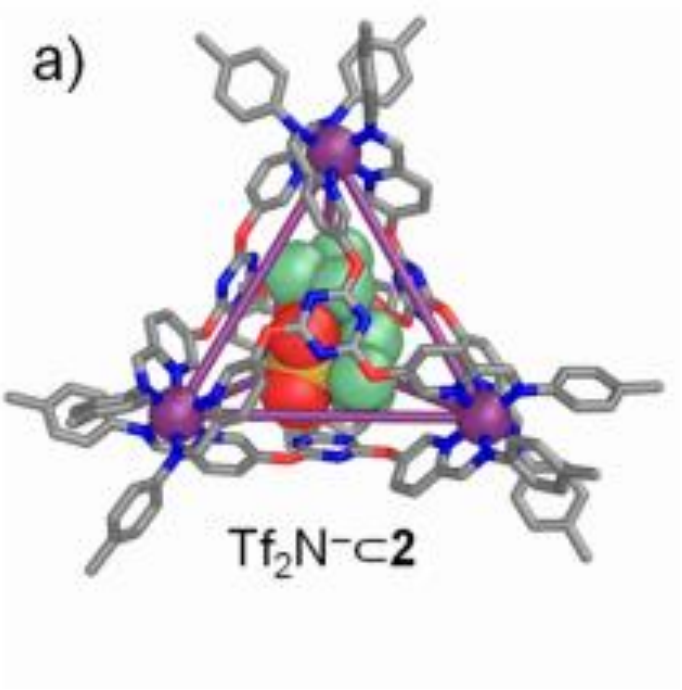

(a) Crystal structure of Tf2N$^-\subset$2. Tf2N$^-$ shown in space-filling mode: N, blue; S, yellow; O, red; C, gray; F, pale green. Disorder, unbound counterions, and solvent of crystallization are omitted for clarity. Attempts to obtain single crystals suitable for X-ray diffraction of an analog of cage 2 with Zn(II) instead of Fe(II) were unsuccessful.

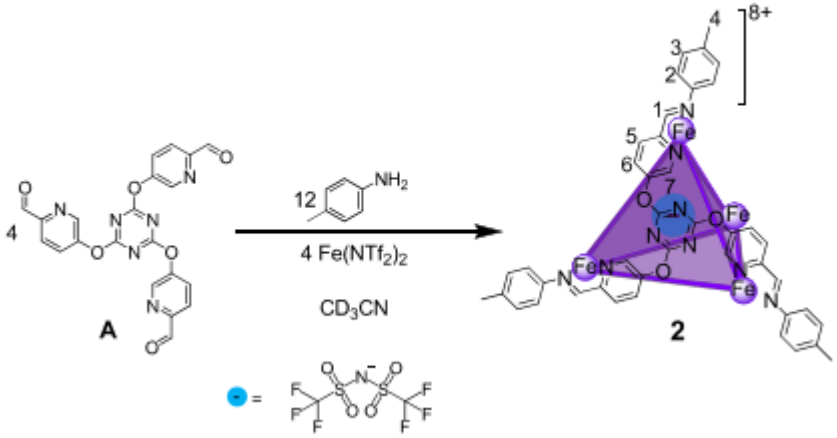

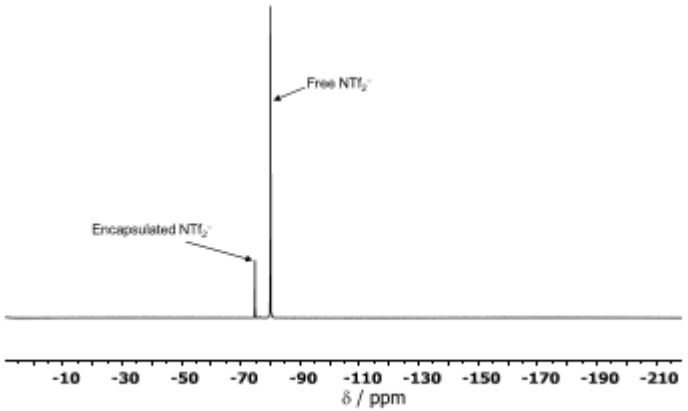

Figure S16. ^{19}F NMR spectrum of $Tf_2N^-\subset$**2** (376 MHz, CD_3CN, 25 °C).

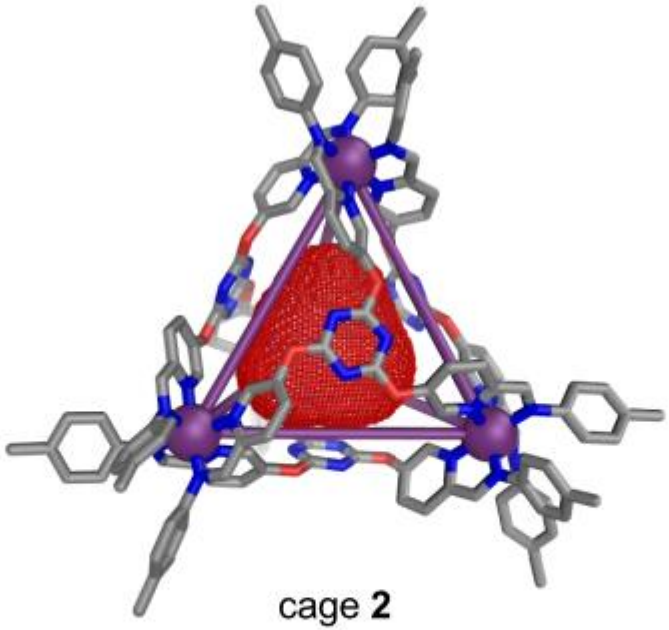

cage **2**

volume = 205 Å^3

Figure S70. MoloVol-calculated void space (red mesh) within the crystal structures of cage **2**.

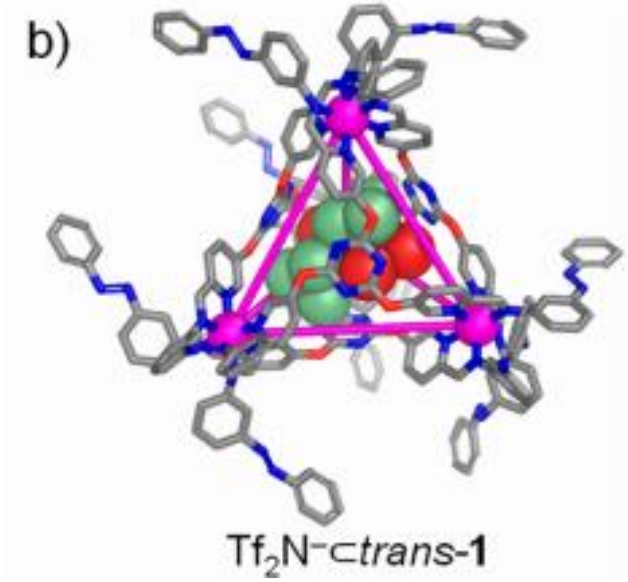

b) MM2-optimized molecular model of ***trans*-1**, based on the structure of **2**.

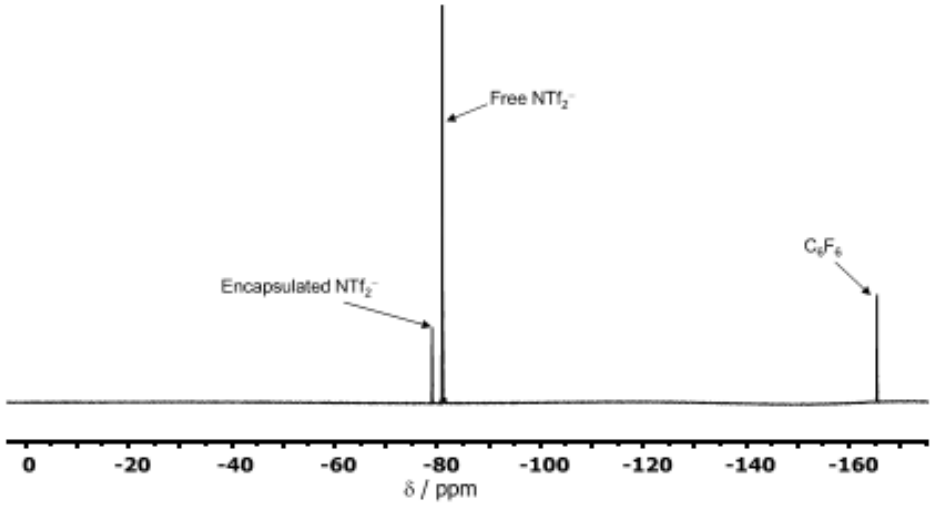

Figure S8. ^{19}F NMR spectrum of Tf_2N^-⊂*trans*-**1** (376 MHz, CD_3CN, 25 °C).

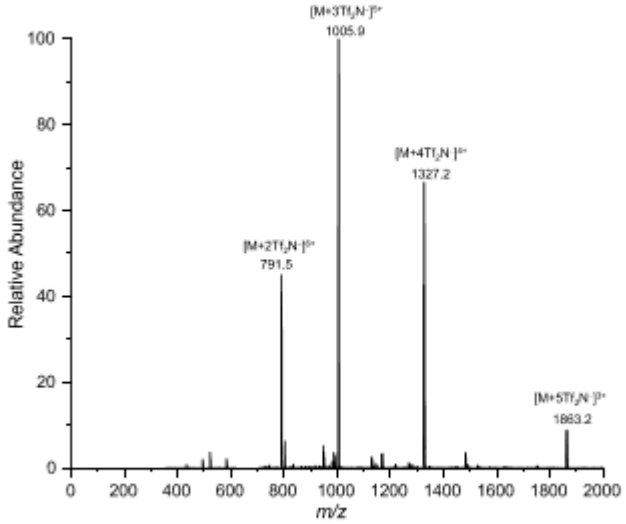

Figure S9. Low-resolution ESI-mass spectrum of Tf_2N^-⊂*trans*-**1** in CH_3CN.

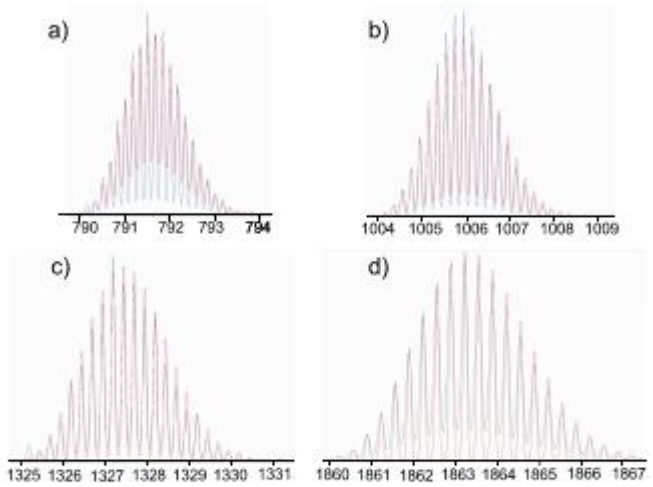

Figure S10. High-resolution ESI-MS spectra of Tf_2N^-⊂*trans*-**1** in CH_3CN. Experimental (blue) and calculated (red) peaks for a) [**1**-2(NTf_2)]$^{6+}$: *m/z* = 791.4812 (calculated *m/z* = 791.4824), b) [**1**-3(NTf_2)]$^{5+}$: *m/z* = 1005.7605 (calculated *m/z* = 1005.7624), c) [**1**-4(NTf_2)]$^{4+}$: *m/z* = 1327.1812 (calculated *m/z* = 1327.1823), d) [**1**-5(NTf_2)]$^{3+}$: *m/z* = 1862.8807 (calculated *m/z* = 1862.8822).

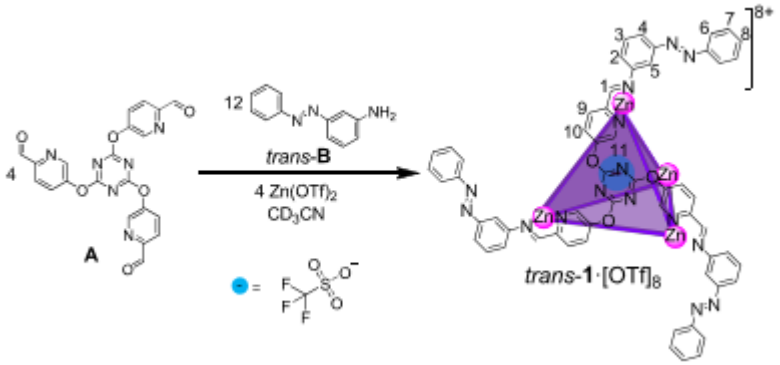

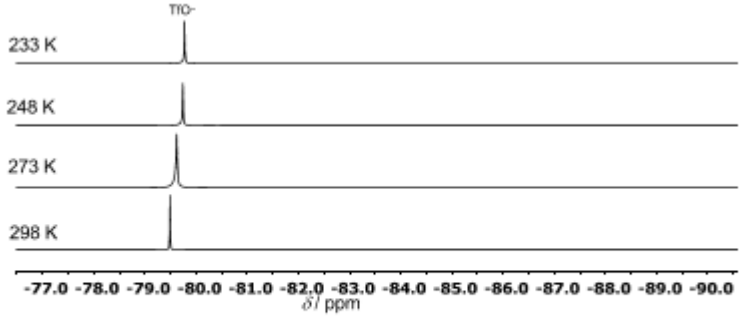

Figure S54. ^{19}F VT-NMR (CD_3CN, 376 MHz) of *trans*-**1**·$[OTf]_8$. With lowering temperature the signals broadened and shifted, suggesting fast exchange of TfO^- within cage *trans*-**1** on the NMR time scale.

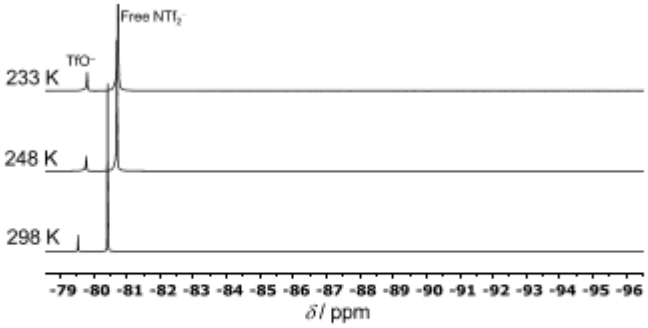

Figure S52. ^{19}F VT-NMR (CD_3CN, 376 MHz) of TfO^-⊂*trans*-**1**. With lowering temperature the signals broadened and shifted, suggesting fast exchange of TfO^- within cage *trans*-**1** on the NMR time scale.

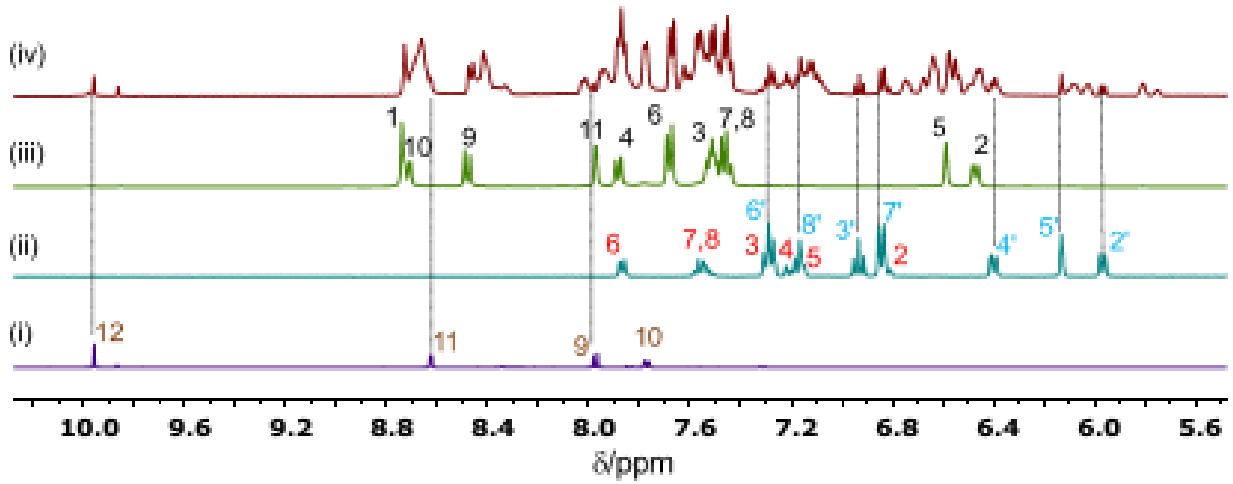

Figure S27. Comparison of ^{1}H NMR spectra (400 MHz, CD_3CN, 25 °C) of (i) subcomponent **A**; (ii) subcomponent **B** after 350 nm irradiation; (iii) pure cage Tf_2N^-⊂*trans*-**1** and (iv) cage Tf_2N^-⊂*trans*-**1** after 350 nm irradiation. The signals of subcomponent **A**, *trans*-**B**, *cis*-**B** and Tf_2N^-⊂*trans*-**1** have been assigned and are indicated by brown, red, cyan and black labels, respectively.

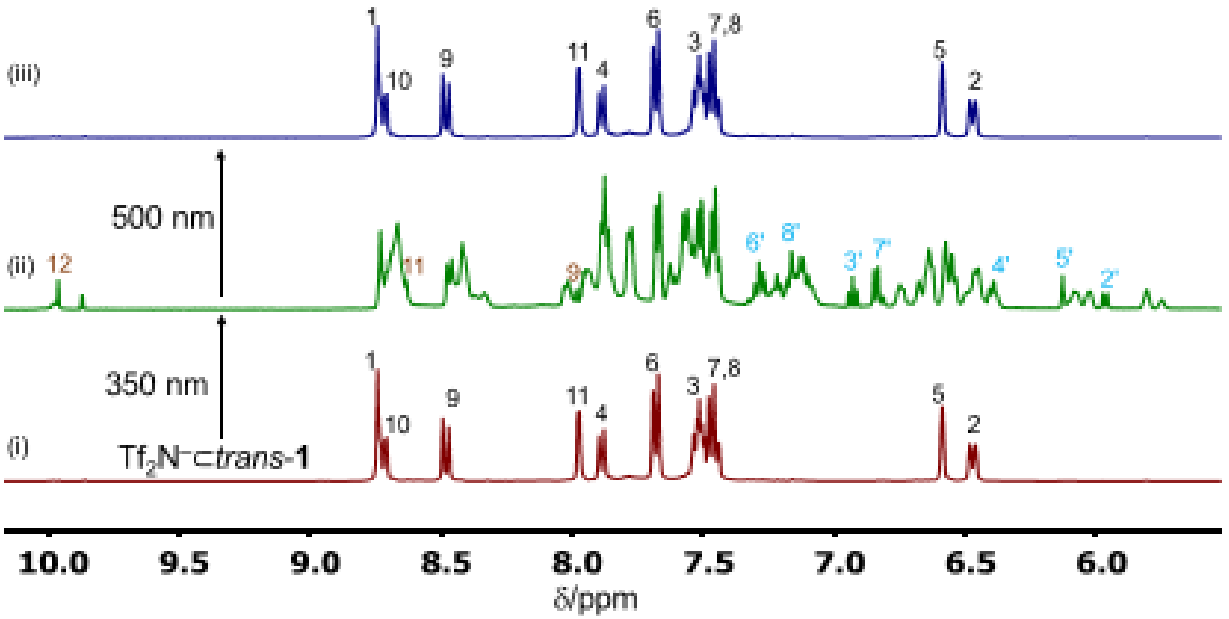

Figure S28. Reversible photoswitching of cage Tf_2N^-⊂*trans*-1 (*c* = 39.6 mM). ^{1}H NMR spectra (500 MHz, CD_3CN, 25 °C) of (i) cage Tf_2N^-⊂*trans*-**1**; (ii) after 350 nm irradiation for 10 min and (iii) after irradiation at 500 nm for 30 min.

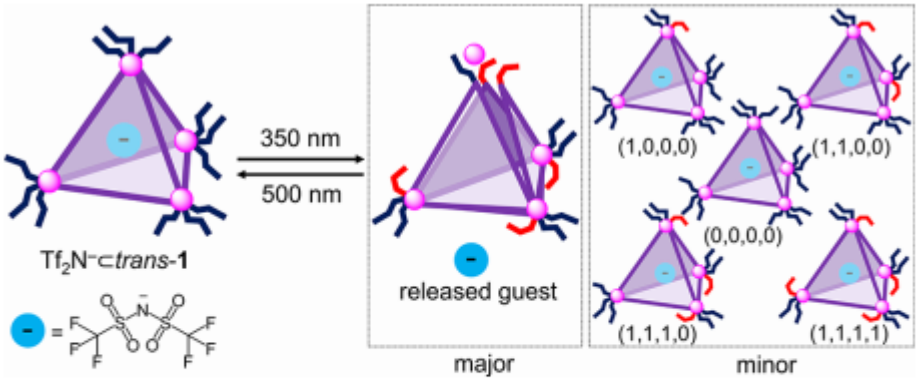

Figure 3. Cartoon of the photoswitching of cage Tf_2N^-⊂*trans*-**1**, illustrating the opening of the cage after a fifth azobenzene switches, along with the five observed guest-binding states of the cage, in which 0–4 azobenzene residues have switched to *cis*. **B** residues with the *trans* and *cis* configurations are colored blue and red, respectively.

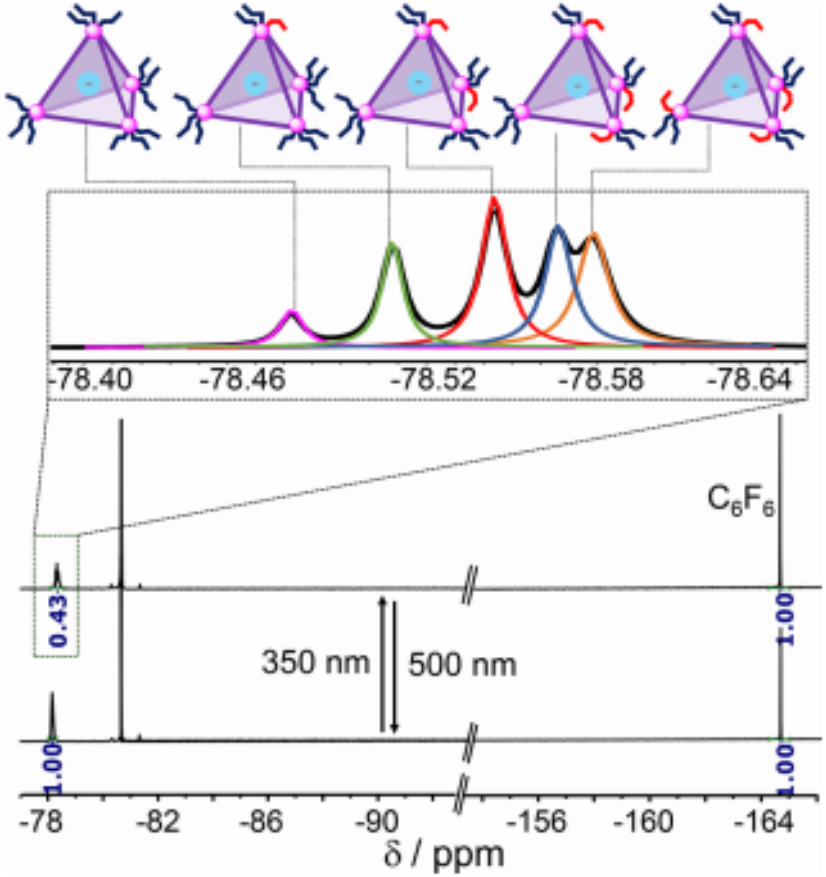

Figure 4. ^{19}F NMR spectra (CD_3CN, 376 MHz, 298 K) show 43% encapsulated/57% released Tf_2N^- guest after UV irradiation for 10 min; the encapsulated Tf_2N^- is quantified by NMR integration with respect to hexafluorobenzene as an internal standard. The five distinct guest-encapsulating cages, incorporating 0–4 *cis*-azobenzene residues, gave rise to five ^{19}F NMR signals, which were deconvoluted as shown.

						Total (%)
Population of *trans* diazo moieties (%)	2	7.3	10.8	7.5	6.7	34.3
Population of *cis* diazo moieties (%)	0%	0.7	2.2	2.5	3.3	8.7

Figure S34. Population of *trans* (34.3%) and *cis* (8.7%) diazo moieties in the 43% of intact, triflimide-binding cages following UV irradiation. After UV irradiation, a total of six peaks appear in the ^{19}F NMR, with five corresponding to bound Tf_2N^- (43%) and one corresponding to free Tf_2N^- (57% released from a cage, along with the unbound counter anions). This 43% / 57% split thus corresponds to the proportion of ligand bound up into cages, vs. free ligand corresponding to cages that have opened. From the 43% of ligand incorporated into cages, we can calculate the amount of isomerization (34.3% *trans* and 8.7% *cis*), but we were unable to quantify the degree of isomerization among the other 57%.

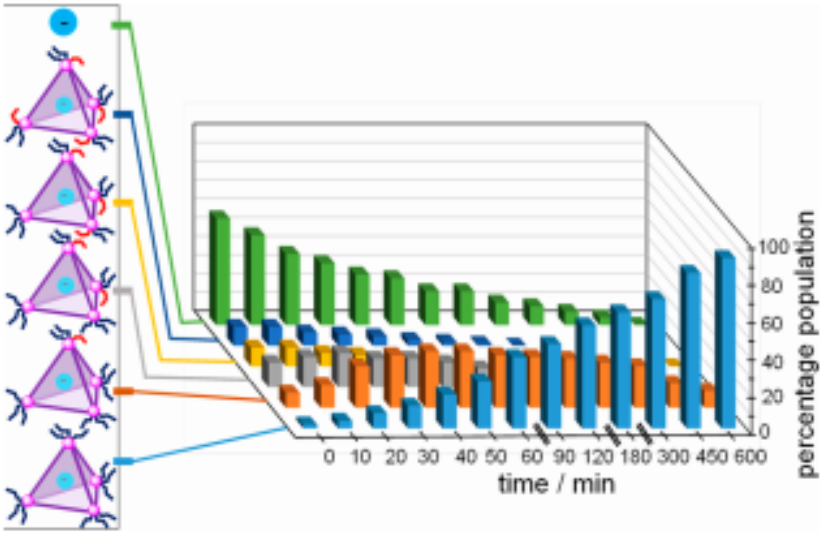

Figure 5. Re-formation of cages incorporating progressively more residues of *trans*-**B** during thermal relaxation while heating to 75 °C, derived from integration of ^{19}F NMR spectra of the encapsulated triflimide guest (Supporting Information, Figure S30). The percentage population value shown is normalized to the maximum amount of anion that can be encapsulated.

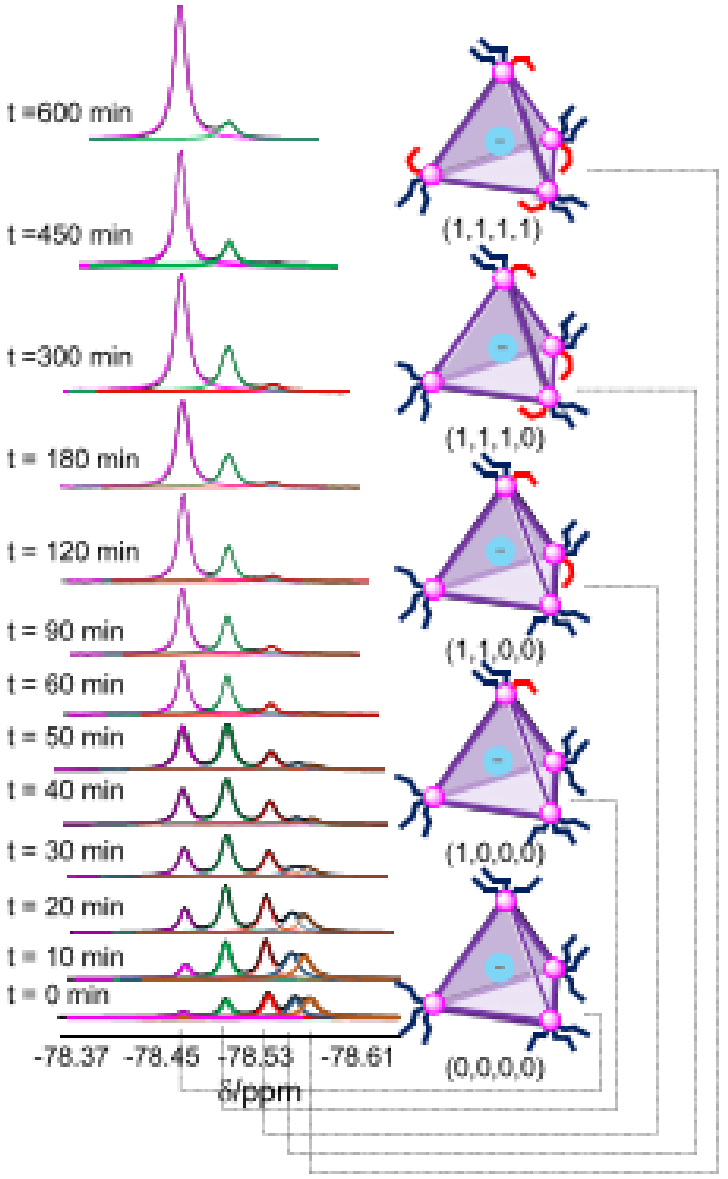

Figure S30. ^{19}F NMR spectra (376 MHz, CD_3CN, 25 °C) of $Tf_2N^-\subset$*trans*-**1** (39.6 mM) at the indicated times during 75 °C heating after 350 nm UV irradiation. Deconvolution of peak clusters with calculated Lorentzian peaks are color coded. The peak at –78.47 (magenta), -78.51 (green), -78.54 (red), -78.57 (blue), and -78.58 (brown) represent Tf_2N^- encapsulated within cages incorporating 0, 1, 2, 3, and 4 *cis* diazo moieties, respectively. The speciation profile in Figure 5 was extracted from this experiment.

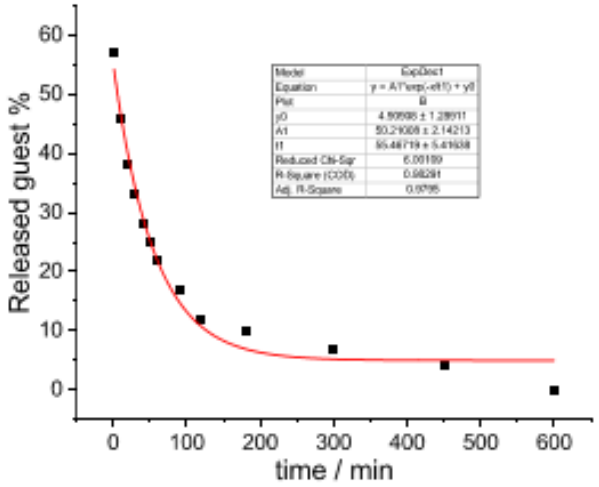

Figure S32. Kinetics for the guest uptake process during reverse photoisomerization towards *trans*-**1** at 75 °C, monitored by integration of encapsulated Tf_2N^- with respect to hexafluorobenzene (Figure S27). The fitting following a 1st order kinetics (red line), revealing a half-life of $t_{1/2}$ = 38 min and rate constants of k = 3.50 x 10^{-4} s^{-1}.

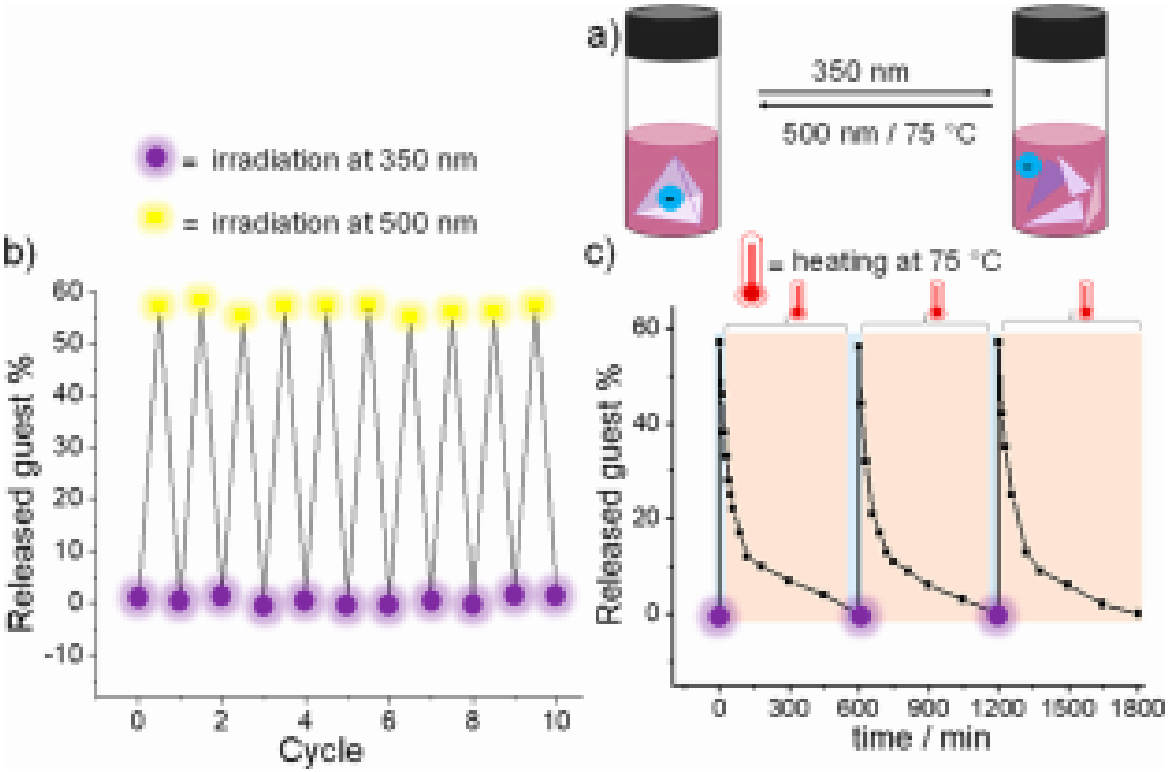

Figure 6. a) Cartoon representation of reversible release and uptake of Tf_2N^- guest by UV light and visible light or heat. b) Ten cycles of guest release driven by irradiation at 350 and 500 nm in CD_3CN in an alternating sequence. c) Three such cycles using light (350 nm) and temperature (75 °C) as stimuli; in both cases no evidence of fatigue was observed.

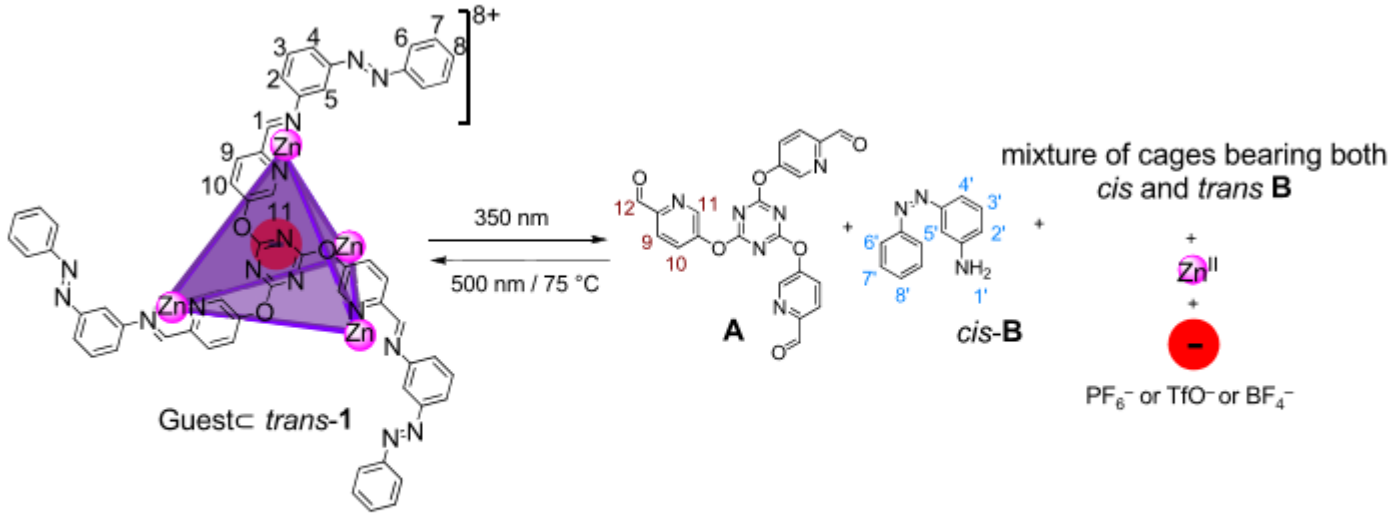

Figure S59. Disassembly and assembly of cage Guest⊂*trans*-**1** and subsequent guest (PF_6^-/TfO^-/ BF_4^-) release and uptake.

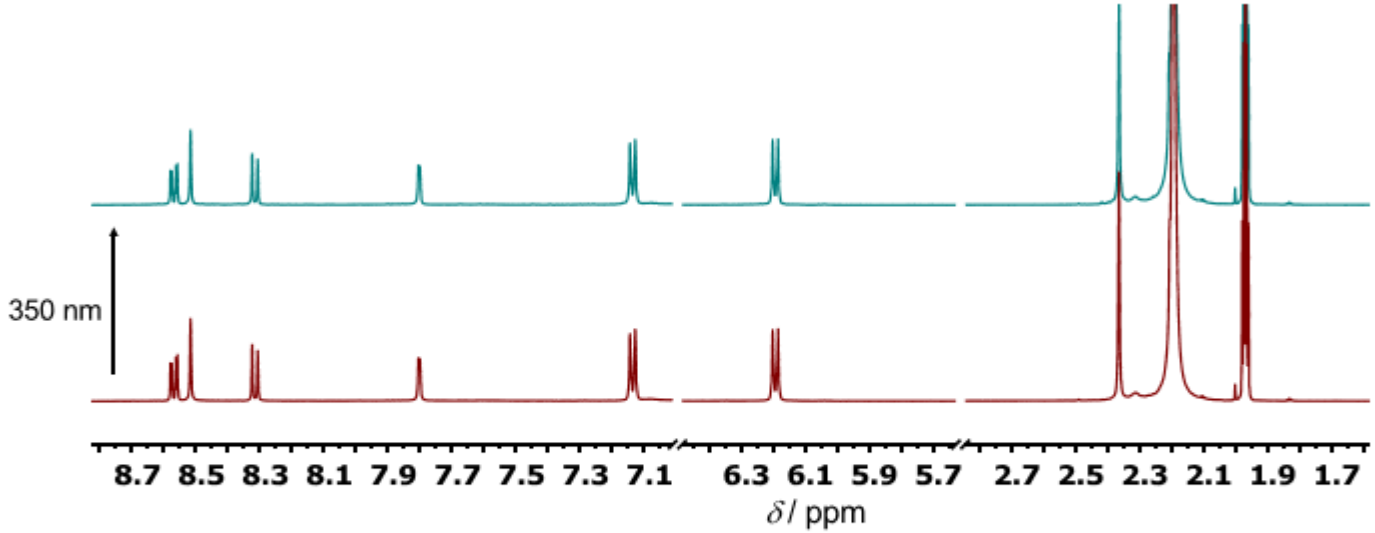

Figure S76. ^{1}H NMR (500 MHz, CD_3CN, 25 °C) of a model cage (cage **2** with Zn^{II} instead of Fe^{II}) before and after UV light irradiation. No disassembly was observed, in contrast with cage *trans*-**1**.

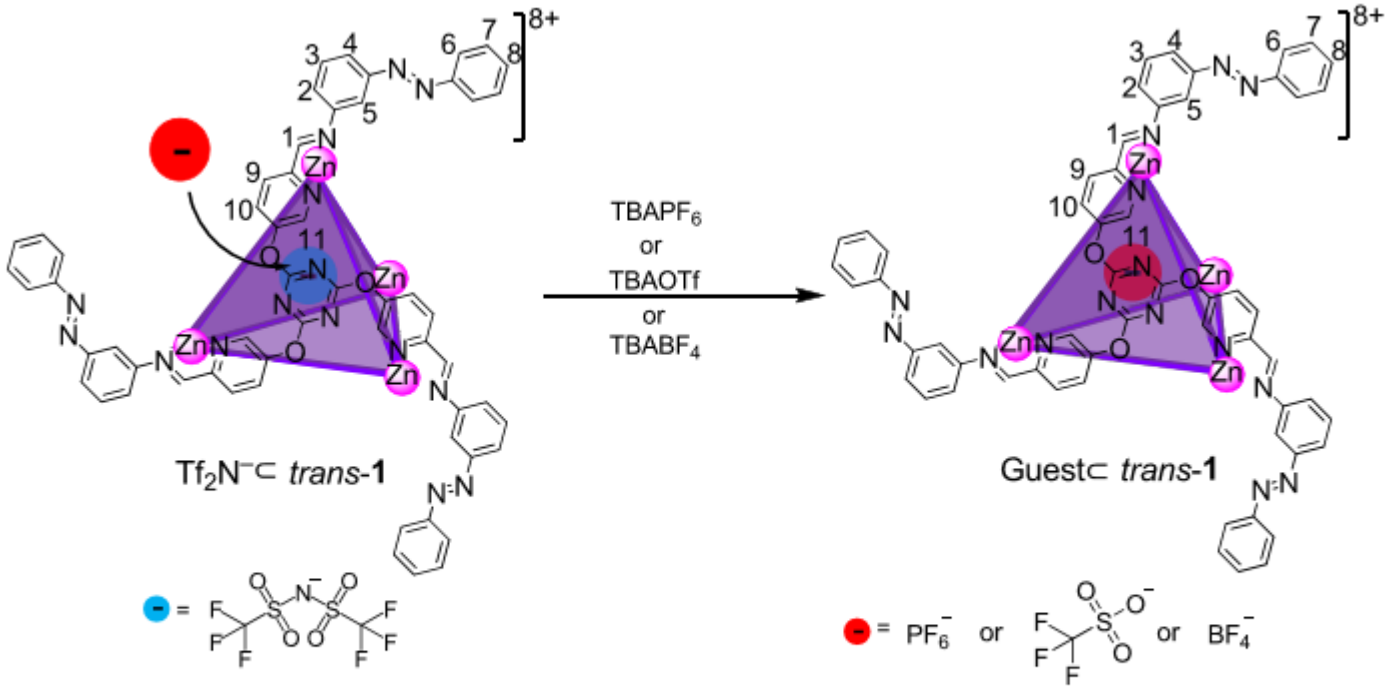

Figure S36. Encapsulation of other anionic guests (PF_6^-, TfO^- and BF_4^-) with subsequent release of Tf_2N^-.

Anion	Volume (Å^3)	K_{rel} ($K_a{}^2/K_{Tf2N^-}$)
Tf_2N^-	131	-
PF_6^-	90	0.15
TfO^-	86	0.11
BF_4^-	50	0.04

Table S2. Reported volumes[2,3] and relative binding affinities of the anions.